THE JOURNAL OF BIOLOGICAL CHEMISTRY VOL. 285, NO. 39, pp. 30224–30232, September 24, 2010

Yeast Lipids Can Phase-separate into Micrometer-scale Membrane Domains*

Received for publication, March 15, 2010, and in revised form, June 9, 2010 Published, JBC Papers in Press, July 20, 2010, DOI 10.1074/jbc.M110.123554

Christian Klose[‡], Christer S. Ejsing[§], Ana J. García-Sáez[¶1], Hermann-Josef Kaiser[‡], Julio L. Sampaio[‡], Michal A. Surma[‡], Andrej Shevchenko[‡], Petra Schwille[¶], and Kai Simons[‡2]

From the [‡]Max Planck Institute of Molecular Cell Biology and Genetics, Pfotenhauerstrasse 108, 01307 Dresden, Germany, the [§]Department of Biochemistry and Molecular Biology, University of Southern Denmark, Campusvej 55, 5230 Odense, Denmark, and the [¶]Institute for Biophysics, Biotechnology Center (BIOTEC), Technische Universität Dresden, Tatzberg 47-51, 01307 Dresden, Germany

The lipid raft concept proposes that biological membranes have the potential to form functional domains based on a selective interaction between sphingolipids and sterols. These domains seem to be involved in signal transduction and vesicular sorting of proteins and lipids. Although there is biochemical evidence for lipid raft-dependent protein and lipid sorting in the yeast *Saccharomyces cerevisiae*, direct evidence for an interaction between yeast sphingolipids and the yeast sterol ergosterol, resulting in membrane domain formation, is lacking. Here we show that model membranes formed from yeast total lipid extracts possess an inherent self-organization potential resulting in liquid-disordered-liquid-ordered phase coexistence at physiologically relevant temperature. Analyses of lipid extracts from mutants defective in sphingolipid metabolism as well as reconstitution of purified yeast lipids in model membranes of defined composition suggest that membrane domain formation depends on specific interactions between yeast sphingolipids and ergosterol. Taken together, these results provide a mechanistic explanation for lipid raft-dependent lipid and protein sorting in yeast.

The membranes that surround the various organelles of eukaryotic cells have distinct lipid compositions. For example, the concentration of sphingolipids and sterols increases along the secretory pathway, being lowest in the endoplasmic reticulum and highest at the plasma membrane (1–3). The major sorting station for vesicular transport of proteins and lipids within the cell is the *trans*-Golgi network (4). Here, clusters of sphingolipids and sterols as well as proteins have been proposed to be involved in the formation of secretory vesicles (SVs)[3] (5, 6). These clusters, called lipid rafts, were proposed to form by the preferential interaction between lipids containing saturated acyl chains, especially (glyco-) sphingolipids and sterols, and by intermolecular hydrogen bonds between (glyco-) sphingolipids. As compared with bulk cellular membranes, lipid rafts are characterized by a higher acyl chain order and tight packing of lipids (7).

Protein-free model membranes have been widely used to study the self-associative properties of sphingolipids and sterols, which are believed to be responsible for lipid raft formation *in vivo* (8, 9). In model membranes with a lipid composition similar to that of detergent-resistant membranes (DRMs) from mammalian cells, the preferential interaction between sphingolipids and sterols is manifested as the coexistence of two fluid membrane phases, which can be observed microscopically in giant unilamellar vesicles (GUVs) (10–13). More specifically, model membranes produced from equimolar mixtures of sphingomyelin (SM), phosphatidylcholine (PC), and cholesterol show domains in the liquid-disordered (Ld) state that are enriched in PC coexisting with a liquid-ordered (Lo) phase rich in SM and cholesterol, the latter being a defining component of the Lo phase (14, 15). The Lo phase is characterized by a higher acyl chain (conformational) order than the Ld phase. Both phases exhibit translational disorder, *i.e.* the lipid molecules are able to diffuse freely in the plane of the membrane (16, 17).

The yeast *Saccharomyces cerevisiae* has been used as an experimental system to study lipid raft-dependent processes (18, 19). In the present study, the issue whether yeast sphingolipids and ergosterol give rise to fluid/fluid phase coexistence in model membranes is addressed. There is a wealth of information available in the literature supporting the idea of lipid raft-dependent protein and lipid sorting in yeast. Many membrane proteins that are transported along the secretory pathway to the plasma membrane are associated with DRMs (18–21). In analogy to mammalian cells, yeast DRMs are enriched in the sphingolipids inositolphosphoceramide (IPC), mannosyl-inositolphosphoceramide (MIPC), mannosyl-diinositolphosphoceramide (M(IP)2C), and ergosterol (19). Consequently, proper biosynthesis of sphingolipids and/or ergosterol is a prerequisite of plasma membrane delivery of

* This work was supported by EUFP6 "PRISM" Grant LSHB-CT2007-037740, Deutsche Forschungsgemeinschaft "Schwerpunktprogramm1175," Bundesministerium für Bildung und Forschung (BMBF) "BioChance Plus" Grant 0313827, and BMBF "ForMaT" Grant 03FO1212. This work was also supported by a predoctoral stipend from the Max Planck Institute (to C. K.).

[1] Present address: Membrane Biophysics, Max Planck Institute of Metals Research and German Cancer Research Center, BIOQUANT, University of Heidelberg, Im Neuenheimer Feld 267, 69120 Heidelberg, Germany.

[2] To whom correspondence should be addressed. E-mail: simons@mpi-cbg.de.

[3] The abbreviations used are: SV, secretory vesicle; SM, sphingomyelin; IPC, inositolphosphoceramide; PI, phosphatidylinositol; PC, phosphatidylcholine; FCS, fluorescence correlation spectroscopy; LUV, large unilamellar vesicle; GUV, giant unilamellar vesicle; DiD, 1,1′-dioctadecyl-3,3,3′,3′-tetramethylindodicarbocyanine perchlorate; GP, generalized polarization; DRM, detergent-resistant membrane; Ld, liquid-disordered; Lo, liquid-ordered; Rh-DOPE, rhodamine B-dioleoyl-phosphatidyl-ethanolamine; DPH, diphenyl-1,3,5-hexatriene; SL, sphingolipids; Ch, channel; BODIPY, 4,4-difluoro-5,7-dimethyl-4-bora-3*a*,4*a*-diaza-*s*-indacene.

several integral membrane proteins (22–25). Moreover, genes involved in sphingolipid and sterol biosynthesis have been shown to interact genetically, further substantiating the view that they are also interacting functionally (26). Finally, a lipidomic analysis of purified post-Golgi vesicles recently provided direct evidence for the selective sorting of sphingolipids and ergosterol into SVs (27). However, experimental evidence for a selective interaction between yeast sphingolipids and ergosterol resulting in phase separation is lacking. Therefore, total lipid extracts and purified yeast lipids were reconstituted in model membranes and investigated with respect to their phase separation propensity. Both spectroscopic and microscopic methods provided evidence for a selective interaction between yeast sphingolipids and ergosterol. This interaction results in phase separation into membrane domains with Lo- and Ld-like properties. Accordingly, yeast sphingolipids and ergosterol fulfill an important criterion of the lipid raft concept.

EXPERIMENTAL PROCEDURES

Yeast Strains, Media, and Growth Conditions—The yeast strains used in this study were in the BY4741 background (*csg2*::*kanMX4*, *sur2*::*kanMX4*, or *elo3*::*kanMX4* in *MAT*a *his3*Δ *leu2*Δ *met15*Δ *ura3*Δ; EUROSCARF). Yeast strains were grown in complete synthetic medium containing 2% glucose and supplemented with 100 μM inositol at 25 °C.

Reagents—C18-sphingomyelin, palmitoyl-oleyl phosphatidylcholine, cholesterol, and lissamine-rhodamine B-dioleoyl-phosphatidyl-ethanolamine (Rh-DOPE) were from Avanti Polar Lipids. Ergosterol and diphenyl-1,3,5-hexatriene (DPH) were from Sigma. Yeast phosphatidylinositol (PI) was from Larodan Fine Chemicals. The species composition of yeast PI was confirmed to be comparable with the species composition of PI from the wild type yeast strain BY4741 (not shown) (28). 1,1′-Dioctadecyl-3,3,3′,3′-tetramethylindodicarbocyanine perchlorate (DiD) was purchased from Invitrogen. BODIPY-cholesterol was a kind gift of R. Bittman (29). C-laurdan was kindly provided by B. R. Cho (30).

Extraction and Purification of Yeast Lipids—Total lipid extracts were prepared by a two-step chloroform/methanol extraction procedure as described (28). 2000 optical density units (ODu) of yeast cells were harvested, washed in 50 ml of H_2O, and resuspended in 4.5 ml of H_2O. The cells were disrupted by bead beating with zirconia beads (BioSpec Products, Inc.). The lysate was extracted once with 106 ml of chloroform/methanol 17:1 (v/v) at 4 °C for 2 h. The organic phase was collected. The remaining aqueous phase was extracted with 120 ml of chloroform/methanol 2:1 (v/v) at 4 °C for 2 h. The sample was treated as described above, and the organic phase was collected. The 2:1 extraction step was repeated with 90 ml of chloroform/methanol 2:1 (v/v). The organic phases were pooled, and the solvent was evaporated using a rotary evaporator. The lipids were dissolved in 10 ml of chloroform/methanol 2:1 (v/v). Successful extraction was confirmed by thin layer chromatography. Lipid concentration was estimated by phosphate analysis. Alternatively, total lipid extracts were prepared by large scale extraction described below.

To purify IPC, 14,000 ODu of *csg2*Δ cells were subjected to a two-step extraction procedure as described above. Volumes of solvents were scaled up 7-fold, accounting for the higher amount of yeast cells used. Lysates were extracted twice with chloroform/methanol 17:1 (v/v) at 4 °C for 2 h to remove apolar lipids. The remaining aqueous phase was extracted three times with chloroform/methanol 2:1 (v/v) to recover the more polar lipids, including the SLs. The organic phases of the chloroform/methanol 2:1 (v/v) extractions were pooled, and the solvent was evaporated. Lipids were subjected to alkaline hydrolysis in 100 ml of 33% methylamine (in ethanol) for 24 h at 55 °C. Methylamine was evaporated, and the lipids were dissolved in chloroform/methanol 1:1 (v/v). Then, the two-step extraction procedure was repeated, the organic phases of the chloroform/methanol 2:1 (v/v) extractions (containing SLs) were recovered and pooled, and the solvent was evaporated. The lipids were dissolved in chloroform/methanol/water 65:25:4 (v/v/v) to give a total SL extract. For the purification of IPC, liquid column chromatography with Silica Gel 60 (Sigma) as solid phase was performed. The total SL extract (~5 mg of lipid) was loaded onto the column and eluted with 60 ml of chloroform/methanol/water 65:25:4 (v/v/v) followed by 60 ml of chloroform/methanol/water 65:35:8 (v/v/v). Fractions were collected and analyzed by mass spectrometry. IPC-containing fractions were pooled, and the solvent was evaporated. IPC was dissolved in chloroform/methanol 1:2 (v/v). The purity of the preparation was confirmed by thin layer chromatography and mass spectrometry. About 2 mg of IPC were obtained as determined by phosphate analysis.

Formation of GUVs and Confocal Fluorescence Microscopy—GUVs were formed by electro-formation in custom-made Teflon chambers with platinum electrodes having a distance of 5 mm (31). Lipids and fluorescent membrane dyes were mixed in organic solvent. A total of 100 nmol of lipids were loaded onto the platinum electrodes and dried under vacuum. The electrodes were placed into GUV formation chambers filled with 350 μl of 300 mM sucrose solution. Electro-formation was carried out with an alternating field at 1.2 V and 10 Hz at 68 °C. GUVs were detached from the electrodes at 1.2 V and 2 Hz at 68 °C. Samples were cooled slowly to room temperature and added to observation chambers (Lab-Tek chambered coverglass #1 German borosilicate, Nunc) filled with PBS. The observation chambers were blocked before with 2 mg/ml BSA or poly-L-lysine (Sigma). GUVs were observed with a confocal laser-scanning microscope (Zeiss LSM 405/594) with a C-Apochromat 40×/1.2 W corr objective at room temperature.

Two-focus Scanning Fluorescence Correlation Spectroscopy (FCS)—Diffusion measurements by two-focus scanning FCS on GUVs were performed at room temperature (22 °C) on a laser scanning microscope Meta 510 system (Carl Zeiss, Jena, Germany) using a 40× NA 1.2 UV-VIS-IR C-Apochromat water immersion objective as described previously (31, 32). The laser power was 25 microwatts. BODIPY-cholesterol (a dye that partitions equally into Lo and Ld domains) at a concentration of 0.01 mol % was used as fluorescent probe for both the Lo and the Ld phase (29). This ensures that the differences in diffusion measured in the two domains are caused by differences in membrane properties and not by the structure of the fluorescent probe itself. In two-focus scanning FCS, two parallel lines are repeatedly scanned in a perpendicular way through a verti-

cal membrane. The intersections with the membrane give rise to two intensity traces from which the autocorrelation and the spatial cross-correlation curves can be calculated. Auto- and cross-correlation curves were fitted to a two-dimensional elliptical Gaussian model with software written in MATLAB (MathWorks) (32).

C-laurdan Spectroscopy and Microscopy—Membrane order was determined by C-laurdan spectroscopy with large unilamellar vesicles (LUVs) at 23 °C as described by Kaiser *et al.* (33). LUVs were prepared as described (34). In brief, organic solvent was evaporated, and the lipids were rehydrated in 200 μl of liposome formation buffer (50 mM Hepes, 150 mM NaCl, 0.2 mM EDTA, pH 7.25). The samples were incubated at 68 °C, 1000 rpm for 30 min followed by five freeze-thaw cycles (freeze in liquid nitrogen, thaw at 25 °C and 1000 rpm). Liposomes were formed by extrusion at 68 °C using gas-tight syringes (Hamilton), 100-nm Whatman® Nuclepore track-etch membranes (Schleicher and Schuell), Whatman drain discs, and the Avanti mini-extruder (Avanti Polar Lipids). 2 pmol of C-laurdan were used for a total of 40 nmol of lipids. The samples were incubated 15 min at 23 °C before spectra acquisition with a FluoroMax-3 fluorometer (Jobin Yvon Horiba). The instrument settings were: increment = 1 nm; excitation slit = 4 nm; emission slit = 3 nm. No polarizers were used. Measurements were performed in a Quartz cuvette. The sample was excited with a wavelength $\lambda = 385$ nm, and the emission spectrum was recorded from 400 to 550 nm. The background spectrum (obtained with the blank sample) was subtracted from the emission spectra, and the generalized polarization (GP) value was calculated according to

$$GP = (I_{400-460} - I_{470-530})/(I_{400-460} + I_{470-530}) \quad \text{(Eq. 1)}$$

where $I_{400-460}$ is the sum of the fluorescence intensities from $\lambda = 400-460$ nm and $I_{470-530}$ is the sum of the fluorescence intensities from $\lambda = 470-530$ nm.

For C-laurdan microscopy, GUVs were formed, and imaging was carried out as described above. To GUVs corresponding to 15 nmol of lipid, 0.1 nmol of C-laurdan was added. GP images were acquired on a Bio-Rad two-photon setup with a Mira 2000 two-photon laser and a 543 nm laser line using a 60 water immersion objective (NA 1.2). C-laurdan was excited at 800 nm, and the emission was captured using 425/50 (Ch1-low) and 525/70 (Ch1-high) filters. Image processing and analyses were carried out using MATLAB R2006B (MathWorks). GP images were computed according to the following

$$GP = (I_{Ch1} - G^*I_{Ch2})/(I_{Ch1} + G^*I_{Ch2}) \quad \text{(Eq. 2)}$$

where the G-factor served to calibrate the channels. GP images were displayed as two-fold binned heat maps as indicated next to the images (Fig. 6*A*) (33).

DPH Anisotropy Measurements—The main phase transition temperature of IPC was determined by DPH fluorescence anisotropy on unilamellar vesicles as described previously (14). 15 nmol of lipid were dried under vacuum and rehydrated with 70 μl of liposome formation buffer (50 mM Hepes, 150 mM NaCl, 0.2 mM EDTA, pH 7.25) at 68 °C for 60 min followed by five freeze-thaw cycles in liquid nitrogen and at room temperature. DPH was added to a final concentration of 10 μM, and the vesicles were heated slowly to 60 °C and incubated for 30 min in a quartz cuvette. Then, the vesicles were cooled slowly to 4 °C and again heated to 74 °C with a heating rate of 0.4 °C/min. Temperature was controlled with a Thermo-Haake thermostat. DPH fluorescence anisotropy was measured with a FluoroMax-3 fluorescence spectrometer (Jobin Yvon Horiba). The samples were excited with 345 nm light, and the fluorescence at 427 nm was detected with an integration time of 0.2 s. The main phase transition temperature was defined by the midpoint of a sigmoid fit to the anisotropy *versus* temperature curve (35).

RESULTS

GUVs from Yeast Total Lipid Extracts Show Micrometer-scale Phase Separation—Membranes with a complex lipid composition have been shown to possess an inherent organizational heterogeneity caused by the preferential interaction between certain lipids. This heterogeneity may be manifested in micrometer-scale phase separation within the membrane bilayer. Dietrich *et al.* (11) showed that model membranes formed from purified brush border membranes exhibit fluid/fluid phase coexistence below 45 °C. Furthermore, chemically induced giant plasma membrane vesicles derived from rat basophilic leukemia (RBL) mast cells can separate into two coexisting fluid phases at temperatures between 10 and 25 °C (36). Finally, plasma membranes have been shown to have the compositional capacity for a raft-based and sterol-dependent membrane phase separation at physiologically relevant temperature (37). If there are lipid species within the yeast lipidome that preferentially interact with one another to facilitate the formation of membrane rafts, one would predict that model membranes of yeast lipid extracts should show properties similar to that of membranes made of lipids from mammalian cells.

To test this prediction, GUVs were formed from total lipid extracts of yeast cells. As revealed by confocal fluorescence microscopy at 23 °C, the GUVs were homogenously labeled with BODIPY-cholesterol, which distributes similarly between the Lo and the Ld phases (Fig. 1*A*). However, a significant proportion of vesicles (~10%) showed domains enriched in DiD, a marker for the Ld phase, coexisting with domains that excluded this dye. The partitioning of the dyes between the two membrane domains implied the coexistence of two fluid-like membrane phases. To confirm this assumption, the translational diffusion of BODIPY-cholesterol in both membrane domains was determined by two-focus scanning FCS (Fig. 1, *B* and *C*) (32). In the DiD-enriched domain, BODIPY-cholesterol diffused with $D = 3.1$ $\mu m^2/s$ (±0.2, S.E.). In contrast, BODIPY-cholesterol diffused with $D = 0.13$ $\mu m^2/s$ (±0.02, S.E.) in the DiD-depleted domain. Both values are in agreement with diffusion coefficients reported for the Ld and the Lo phase, respectively (38). Therefore, the yeast lipidome contains species that facilitate Ld-Lo phase coexistence.

Defects in Sphingolipid Metabolism Reduce Membrane Order and Prevent Phase Separation—According to the lipid raft concept, the selective interaction between sphingolipids and sterols result in the formation of biologically active membrane domains (5, 8). To ascertain whether yeast sphingolipids are

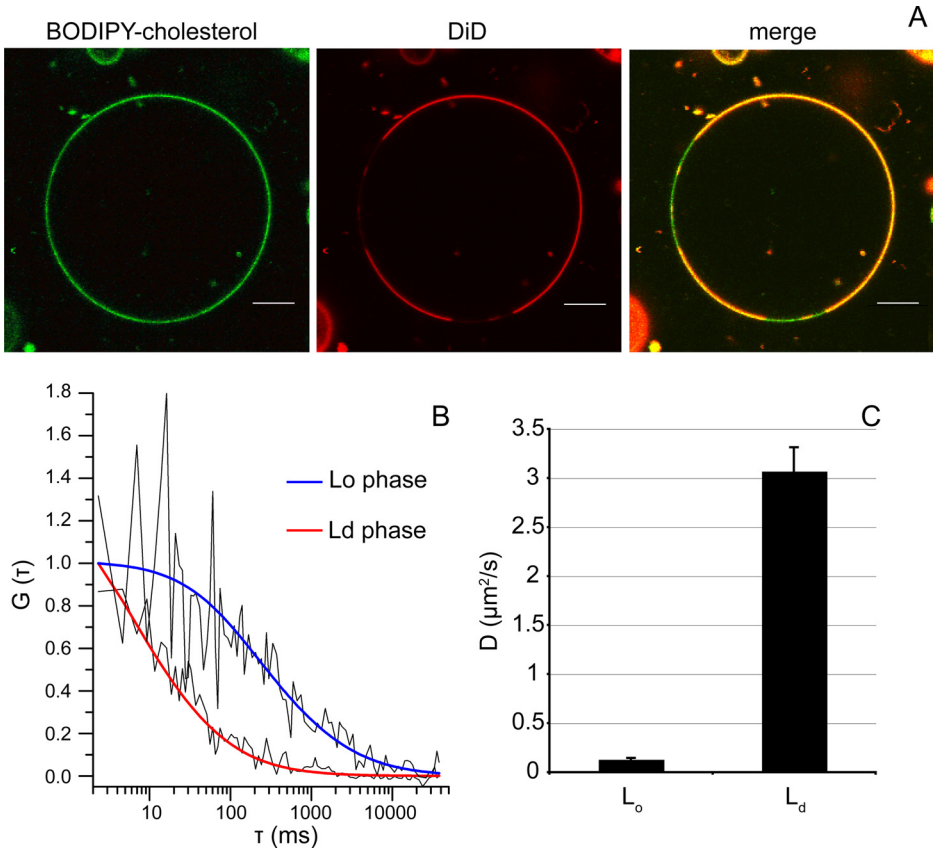

FIGURE 1. **GUVs from total lipid extracts show micrometer-scale phase separation.** DiD (0.1 mol %) was used as marker for the Ld phase (*red*), whereas BODIPY-cholesterol (0.1 mol %) distributes uniformly in the bilayer (*green*). *A*, DiD is excluded from certain areas of the GUV as revealed by confocal fluorescence microscopy (*scale bars* = 10 μm). *B*, autocorrelation curves obtained by two-focus scanning FCS. Curves for the Ld phase (*red*) were obtained from areas of the GUVs that were labeled with DiD (0.1 mol %). Curves for the Lo phase were obtained from areas excluding DiD. Curves were recorded by detecting BODIPY-cholesterol (0.01 mol %). *C*, the diffusion coefficients calculated were D(Lo) = 0.13 (±0.02) and D(Ld) = 3.1 (±0.2) (± S.E.; $n \geq 28$).

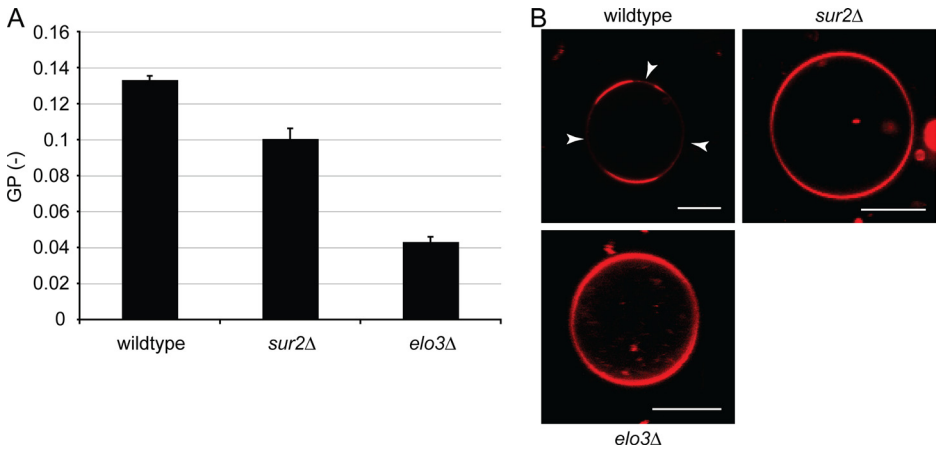

FIGURE 2. **Total lipid extracts from sphingolipid metabolism mutants exhibit altered membrane properties.** *A*, C-laurdan spectroscopy with LUVs from total lipid extracts. LUVs from extracts of the sphingolipid metabolism mutants *sur2*Δ (GP = 0.1; ±0.006) and *elo3*Δ (GP = 0.043; ±0.003) have a reduced order as compared with wild type (GP = 0.133; ±0.002). *Error bars* indicate S.E. ($n = 3$). The differences are statistically significant ($p < 0.05$ for *sur2*Δ *versus* wild type and $p < 0.01$ for *elo3*Δ *versus* wild type). *B*, GUVs formed from the same extracts as in *A* visualized by confocal fluorescence microscopy. Membranes were labeled with the Ld phase marker DiD (0.1 mol %). *Arrowheads* indicate membrane domains that exclude DiD. No phase separation could be observed in GUVs made from *sur2*Δ and *elo3*Δ extracts. *Scale bars*: wild type = 10 μm; *sur2*Δ = 20 μm; *elo3*Δ = 10 μm.

involved in phase separation, we characterized model membranes made from lipid extracts of the sphingolipid metabolism mutants *sur2*Δ and *elo3*Δ. Deletion of *ELO3*, the gene encoding a fatty acid elongase, results in depletion of C26 very long chain fatty acids as well as reduced levels of sphingolipids (28, 39). *SUR2* encodes the hydroxylase responsible for the conversion of dihydrosphingosine to phytosphingosine. Its deletion results in sphingolipids lacking the C4 hydroxylation of the sphingoid base moiety (40).

The mutant total lipid extracts were used for the formation of LUVs and subsequent C-laurdan spectroscopy. C-laurdan is a fluorescent probe that exhibits a fluorescence emission spectrum that is sensitive to lipid packing (30, 33). From the emission spectrum, one can calculate a GP value that can theoretically assume values between −1 and 1; a high GP value reflects ordered membranes, whereas a low GP value is indicative of more disordered membranes (33). LUVs from wild type total lipid extract have a GP = 0.133 (Fig. 2*A*). Notably, LUVs produced from *sur2*Δ total lipid extracts exhibit a significantly lower GP value (0.101), suggestive of a lower membrane order. The membrane order is even further decreased in LUVs made from *elo3*Δ extracts, as reflected by a GP value of 0.043. The reduced membrane order in these mutants was not caused by the accumulation of free long chain bases (28) because the addition of exogenous long chain bases did not affect membrane properties of liposomes formed from wild type lipid extracts (not shown). To examine whether defects in sphingolipid metabolism also affect the propensity of the membranes to exhibit phase separation, GUVs were formed from mutant total lipid extracts. Interestingly, neither GUVs from *sur2*Δ extracts nor GUVs from *elo3*Δ extracts showed phase separation (Fig. 2*B*).

Taken together, lipid extracts from mutant yeast strains with defective sphingolipid biosynthesis and a concomitantly perturbed sphingolipid composition confer a decreased order of model membranes, which is accompanied by the inability to promote micrometer-scale phase sep-

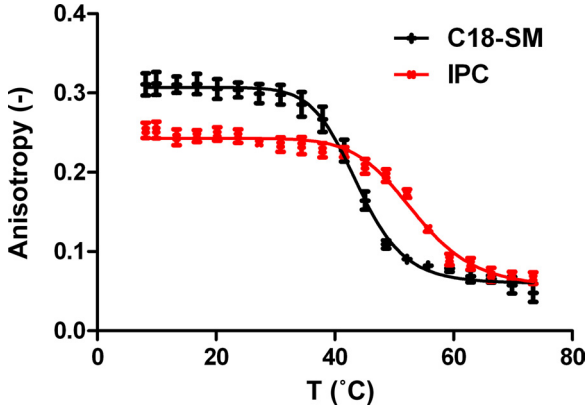

FIGURE 3. **Phase transition temperature of IPC.** Phase transition temperatures (T_m) were determined by DPH fluorescence anisotropy measurements as described under "Experimental Procedures." The T_m of IPC was determined to be 53.4 °C (±0.2; S.E.; *red*). As a control, the T_m of C18-SM was determined (T_m = 44.0 °C; ±0.1; S.E.; *black*). (n = 3).

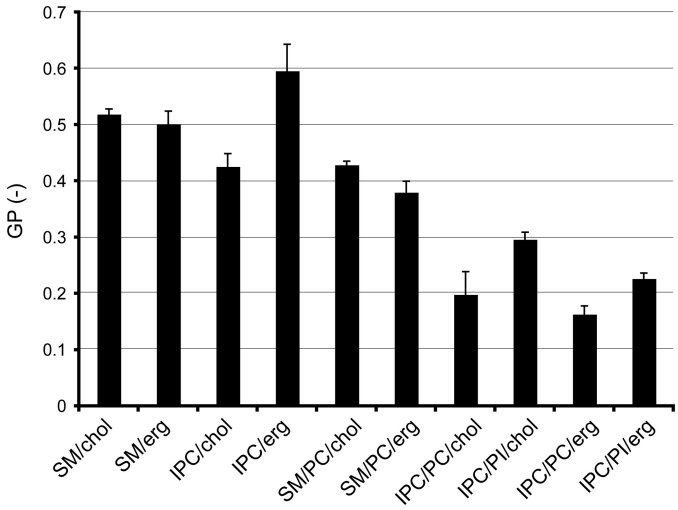

FIGURE 4. **IPC and ergosterol form ordered membranes.** Membrane order was measured by C-laurdan spectroscopy of LUVs consisting of binary and ternary equimolar lipid mixtures. *Error bars* indicate S.E. ($n \geq 3$). *SM* = C18-SM; *chol* = cholesterol; *erg* = ergosterol; *PI* = yeast PI; *PC* = palmitoyl-oleyl phosphatidylcholine.

aration. These results imply a direct role of yeast sphingolipids in the formation of membrane domains.

Phase Transition Temperature of Purified IPC—To more directly address the question whether yeast sphingolipids are involved in the phase separation observed in vesicles made of total lipid extracts, membranes of simpler compositions were investigated. To this end, we purified IPC, one of the major yeast sphingolipids. As an initial characterization, the main phase transition temperature (T_m) of IPC was determined by DPH fluorescence anisotropy. At the T_m, lipids undergo a transition from the gel/solid-ordered phase (where the lateral mobility of the lipids is restricted and their acyl chains are tightly packed) to the Ld phase (41). The "melting" of the gel phase is reflected by a temperature-dependent reduction of the fluorescence anisotropy of the dye DPH. T_m was defined as the midpoint of the sigmoid anisotropy *versus* temperature curve (Fig. 3, see also "Experimental Procedures"). As a comparison, the T_m of C18-SM was determined to be 44.0 °C. This value is in agreement with previous reports (14, 42). The T_m of IPC was 53.4 °C. This difference in T_m probably reflects a tighter packing of IPC molecules in the gel phase as compared with SM.

Characterization of Model Membranes with Defined Compositions of Yeast Lipids—Next, we undertook a systematic investigation of the properties of yeast lipids and their impact on membrane order. To this end, we made binary and ternary lipid mixtures of IPC, yeast PI, and ergosterol similar to the well characterized model membrane mixtures of mammalian SM, cholesterol, and PC (14, 33, 38). Yeast PI was used because it is the most abundant glycerophospholipid in yeast and it is enriched in SVs (27, 28). The membrane order was determined by C-laurdan spectroscopy (Fig. 4). In equimolar binary mixtures of sphingolipids and sterols, replacement of cholesterol by ergosterol had no influence on membrane order (Fig. 4; compare SM/cholesterol (*SM/chol*) with SM/ergosterol (*SM/erg*)). However, exchange of SM with IPC led to a decrease in membrane order (SM/cholesterol *versus* IPC/cholesterol). LUVs composed of IPC and ergosterol (*IPC/erg*) showed the highest GP value among all compositions tested.

When SM, PC, and cholesterol in equimolar ternary mixtures were substituted by IPC, yeast PI, and ergosterol, respectively, three major observations were made. (i) In the presence of SM, replacement of cholesterol by ergosterol results in a membrane order that is as high as the order of membranes of the well characterized raft mixture SM/PC/cholesterol. This result confirms previous reports showing the property of ergosterol to have a condensing effect on glycerophospholipids (43–46). (ii) Yeast PI increases the order of membranes containing IPC, irrespective of whether cholesterol or ergosterol is used as the sterol in these mixtures. Notably, this effect is most significant for IPC/yeast PI/ergosterol (compare with IPC/PC/ergosterol). (iii) IPC-containing membranes have a lower order than membranes containing SM. However, their order is considerably higher than that of pure PC vesicles, which are *bona fide* Ld membranes and give rise to negative GP values (33).

GUVs Containing IPC/PI/Ergosterol Show Lo-Ld Phase Separation—The GP value measured for IPC/yeast PI/ergosterol suggests that this mixture has the capacity to promote phase separation. Therefore, we tested whether this mixture would phase-separate in GUVs. GUVs composed of IPC/yeast PI/ergosterol 1:1:1 (molar ratio) were formed and visualized by confocal fluorescence microscopy. Importantly, the GUVs showed prominent micrometer-scale phase separation. Domains that exclude the Ld phase marker DiD coexist with domains that are labeled by DiD (Fig. 5*A*). To ensure that the domains are present in the fluid Lo- and Ld-like states, respectively, two-focus scanning FCS was performed. The calculated diffusion coefficients confirmed that the DiD-labeled domains are in the Ld-like phase, whereas the DiD-excluding domains are present in the Lo-like phase (Fig. 5, *B* and *C*). However, the diffusion coefficient measured for the Ld-like phase is lower than previously reported values for the Ld phase in GUVs containing SM/DOPC/cholesterol (38). Slower diffusion is indicative of a higher membrane order. To get another measure for order, C-laurdan microscopy was applied to GUVs containing IPC/yeast PI/ergosterol (Fig. 6). The GUVs were labeled with Rh-DOPE, a marker for the Ld-like phase, and with C-laurdan. Again, GUVs were phase-separating in domains that exclude or

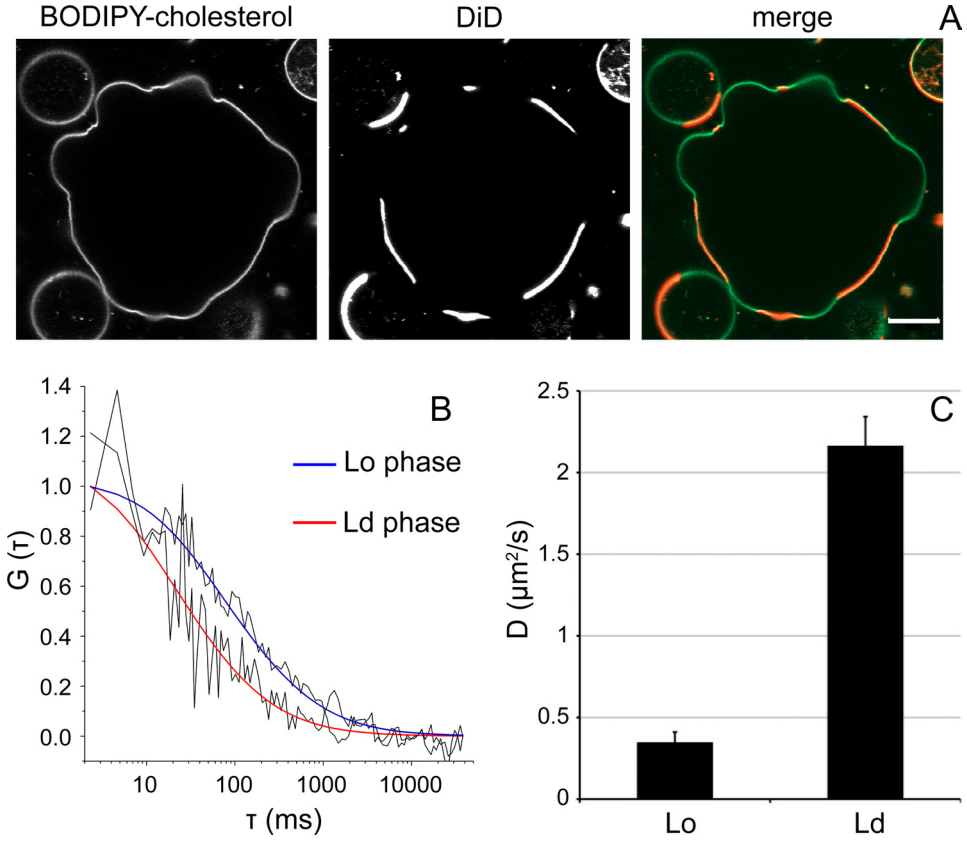

FIGURE 5. **Phase separation of GUVs containing IPC/yeast PI/ergosterol.** *A*, GUVs produced from equimolar mixtures of IPC, yeast PI, and ergosterol show micrometer-scale phase separation as observed by confocal fluorescence microscopy. DiD (0.1 mol %) was used as a marker for the Ld phase, whereas BODIPY-cholesterol (0.1 mol %) labels both the Ld and the Lo phase. DiD is excluded from parts of the GUVs (*scale bar* = 10 μm). *B*, autocorrelation curves obtained by two-focus scanning FCS. Curves for the Ld phase (*red*) were obtained from areas of the GUVs that were labeled with DiD (0.1 mol %). Curves for the Lo phase were obtained from areas excluding DiD. Curves were recorded by detecting BODIPY-cholesterol (0.01 mol %). *C*, the diffusion coefficients calculated were D(Lo) = 0.35 (±0.06) and D(Ld) = 2.2 (±0.2) (± S.E.; $n \geq 4$).

enrich Rh-DOPE, indicating the coexistence of Lo- and Ld-like domains, respectively (Fig. 6*A*, *left*). As shown in the false-colored GP image, a more ordered membrane domain is coexisting with a more disordered domain (Fig. 6*A*, *right*). With GP = 0.79, the ordered phase shows a GP value similar to what has been measured for the Lo phase of SM/DOPC/cholesterol 2:2:1 (molar ratio) (33). In contrast, the GP value of the disordered phase in the yeast system is 0.34, which is considerably higher than the order of the Ld-like phase in the SM/DOPC/cholesterol system (GP = −0.34; (33)), confirming the diffusion measurements and indicating a relatively high order of the Ld-like phase in GUVs produced from IPC/yeast PI/ergosterol. Collectively, the results obtained from two-focus scanning FCS and C-laurdan spectroscopy show that GUVs containing yeast sphingolipids and ergosterol exhibit phase separation into Lo-like domains, thereby supporting the notion that their selective interaction sustains functional lipid rafts in the cellular context.

DISCUSSION

Biophysical studies of lipids have so far focused on a limited number of lipids. Of the specific yeast lipids, only ergosterol has been investigated in detail. The question that we addressed herein was whether yeast sphingolipids and ergosterol are capable of forming membrane domains. We characterized the biophysical properties of model membranes composed of yeast lipids and compared them with the well characterized model membrane system containing mammalian SM, PC, and cholesterol.

Phase Transition Temperature of IPC—As revealed by a decrease in DPH anisotropy, membranes formed from IPC, a major representative of the yeast sphingolipids, undergo a transition from gel phase to Ld phase at 53.4 °C. This value is higher than the T_m of C18-SM (T_m = 44 °C), which was used for comparison throughout this study because its properties in model membranes have been studied in detail (14, 38). A major structural parameter known to have an impact on the phase transition temperature of lipid bilayers is the ability of a lipid to form intermolecular hydrogen bonds with surrounding lipids. Intermolecular hydrogen bonds are mainly formed between the carbonyl and the amide group of SM and the 3-hydroxyl group and the phosphoryl oxygens (47). In comparison with SM, yeast IPC contains additional hydroxyl groups at the 2 position of the amide-linked fatty acid moiety (α-hydroxylation) and at the 4 position of the sphingoid base (*i.e.* phytosphingosine, see structures in Fig. 7) (28). These structural attributes increase the probability of hydrogen bond formation between adjacent lipid molecules, thereby stabilizing the gel phase and presumably resulting in increased phase transition temperature (48). Moreover, yeast sphingolipids contain hydroxyl-rich inositol phosphate headgroups that have a positive effect on the phase transition temperature of lipids. For example, glycosphingolipids have higher phase transition temperatures than non-glycosylated sphingolipids (48). It is therefore reasonable to assume that the inositol headgroup of IPC with five hydroxyl groups is involved in extensive hydrogen bonding (48, 49). This view is supported by a recent study reporting a higher T_m for an inositol phosphate-containing sphingolipid than for an acyl chain-matched SM (50).

Another structural feature of IPC is its hydrocarbon chain asymmetry. As reported for C24-sphingomyelin, hydrocarbon chain asymmetry might result in partially or even mixed interdigitated bilayers in the gel phase (51–53). Interdigitated bilayers are characterized by a complex thermotropic behavior caused by changes in the degree of interdigitation upon heating above the phase transition temperature (51). One might speculate that the rather broad transition from gel to fluid phase observed for IPC is caused by similar transitions between interdigitation states as observed for C24-SM.

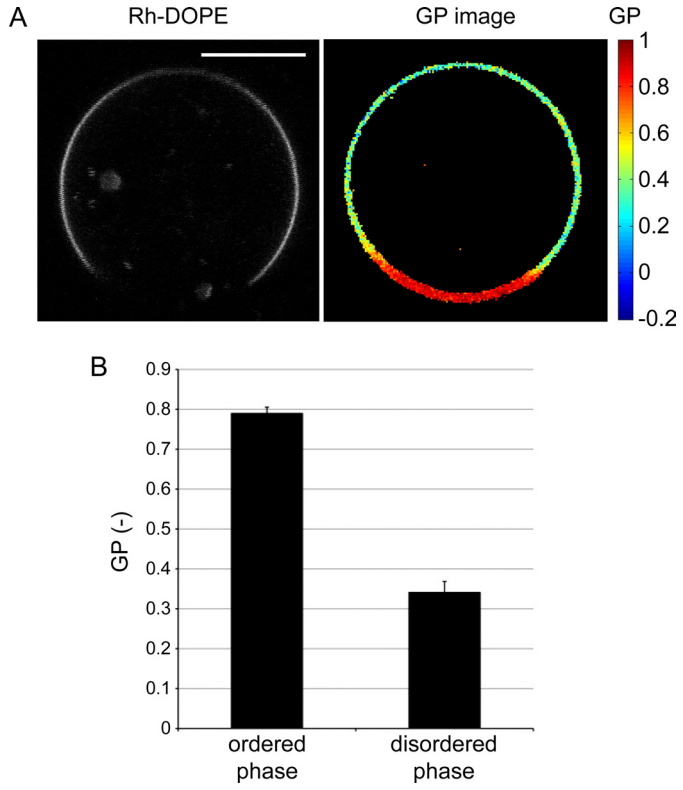

FIGURE 6. **Membrane order of GUVs containing IPC/yeast PI/ergosterol as determined by C-laurdan microscopy.** GUVs as in Fig. 5 were labeled with 0.05 mol % Rh-DOPE as a marker for the Ld phase, stained with C-laurdan, and imaged by two-photon fluorescence microscopy. *A*, GUVs show phase separation as indicated by the exclusion of Rh-DOPE from parts of the GUVs (*scale bar* = 10 μm). The false-colored GP image indicates differences in membrane order of the two domains. The *color bar* indicates the GP values. *B*, C-laurdan GP values as sampled from the GP images. *Error bars* indicate S.E., $n = 3$.

IPC-Ergosterol Interactions—Because the preferential interaction between sphingolipids and sterols is an essential tenet of the lipid raft concept, the next step was to investigate the interaction of IPC with ergosterol (5, 7). Several experimental data indicate a strong tendency of SM and cholesterol to interact with each other, mainly caused by van der Waals attractive forces between the saturated acyl chain of SM and the rigid cholesterol ring backbone (52, 54). In addition, experimental and computational data suggest that hydrogen bonds between SM and cholesterol might facilitate their interaction, presumably via the amide group of SM and the 3-hydroxyl of cholesterol (55, 56). Alternatively, charge pairing between the headgroup nitrogen of SM and the 3-hydroxyl of cholesterol was proposed to be involved in the SM-cholesterol interaction (57, 58). Because the order of IPC/ergosterol membranes is comparable with SM/cholesterol membranes (Fig. 4), the IPC-ergosterol interactions seem to be similar to the interactions described for SM and cholesterol. Although charge pairing is unlikely to occur because the IPC headgroup is negatively charged, van der Waals interactions between the saturated very long fatty acid chain of IPC and ergosterol and hydrogen bonds between the amide group of IPC and the 3-hydroxyl of ergosterol might facilitate their interaction. Moreover, despite the fact that hydrogen bonds between ceramide backbones of SMs are known to be reduced in the presence of cholesterol, IPC-IPC interactions via the headgroup hydroxyl groups might still occur and could potentially increase the condensation state of the bilayer (56). This view is supported by the finding that cholesterol does not increase the distance between the phosphates of adjacent C18-SM molecules and hence is not decreasing the probability of headgroup interactions (56).

Interestingly, the order of IPC/cholesterol bilayers is significantly lower than that of IPC/ergosterol bilayers. However, there is no difference between C18-SM/cholesterol and C18-SM/ergosterol bilayers (Fig. 4). This result implies that ergosterol has some structural properties distinct from cholesterol that are required for the condensation of IPC-containing bilayers. Ergosterol differs from cholesterol in additional double bonds in the B ring and the hydrocarbon side chain and an additional methylation at C24, the latter two making the side chain stiffer and bulkier, respectively (59). These structural attributes were proposed to restrict the motions of acyl chains more efficiently and thus lead to stronger ordering by ergosterol as compared with cholesterol (43–46). As judged from the higher order of IPC/ergosterol membranes, this effect is more pronounced for IPC, whereas the sterol structure does not seem to be critical for the ordering of C18-SM-containing bilayers (Fig. 4). One might speculate that the typical ergosterol structure, *i.e.* the stiff and bulky side chain, is critical for ordering lipids with very long chain fatty acids. In support of this view, a functional relation between ergosterol side chain structure and fatty acid length has been suggested based on the finding that the mutant *erg6*Δ genetically interacts with *elo3*Δ (60). Future experiments will reveal whether the most abundant yeast SL M(IP)2C has similar properties with respect to its interaction with ergosterol and phase separation.

Micrometer-scale Phase Separation in Membranes Containing Yeast Lipids—Model membranes containing SM, PC, and cholesterol exhibit micrometer-scale phase separation into Lo and Ld domains (11, 38). We wanted to determine whether yeast sphingolipids and ergosterol exhibited a similar property. As revealed by C-laurdan spectroscopy (Fig. 4), the membrane order of ternary mixtures containing IPC is similar to that of other phase-separated membrane systems (33). Membranes containing IPC, ergosterol, and PI, the major glycerophospholipid in yeast (28), showed a higher order than bilayers containing PC. This mixture also showed prominent micrometer-scale phase separation, resembling SM/PC/cholesterol-containing GUVs (Figs. 5 and 6) (11, 38). The phase separation property of IPC/yeast PI/ergosterol membranes depends on the presence of IPC because GUVs containing yeast PI/ergosterol (2:1 molar ratio) did not show any phase separation (not shown).

What drives the domain formation in membranes containing IPC, yeast PI, and ergosterol? First, the preferential interaction of IPC with ergosterol via hydrogen bonds and van der Waals interactions between the very long saturated fatty acid and the rigid sterol ring backbone could be important. IPC might be preferred over yeast PI because the most abundant yeast PI species comprise an unsaturated fatty acid, which is probably unfavorable for an interaction with ergosterol (28, 46). Second,

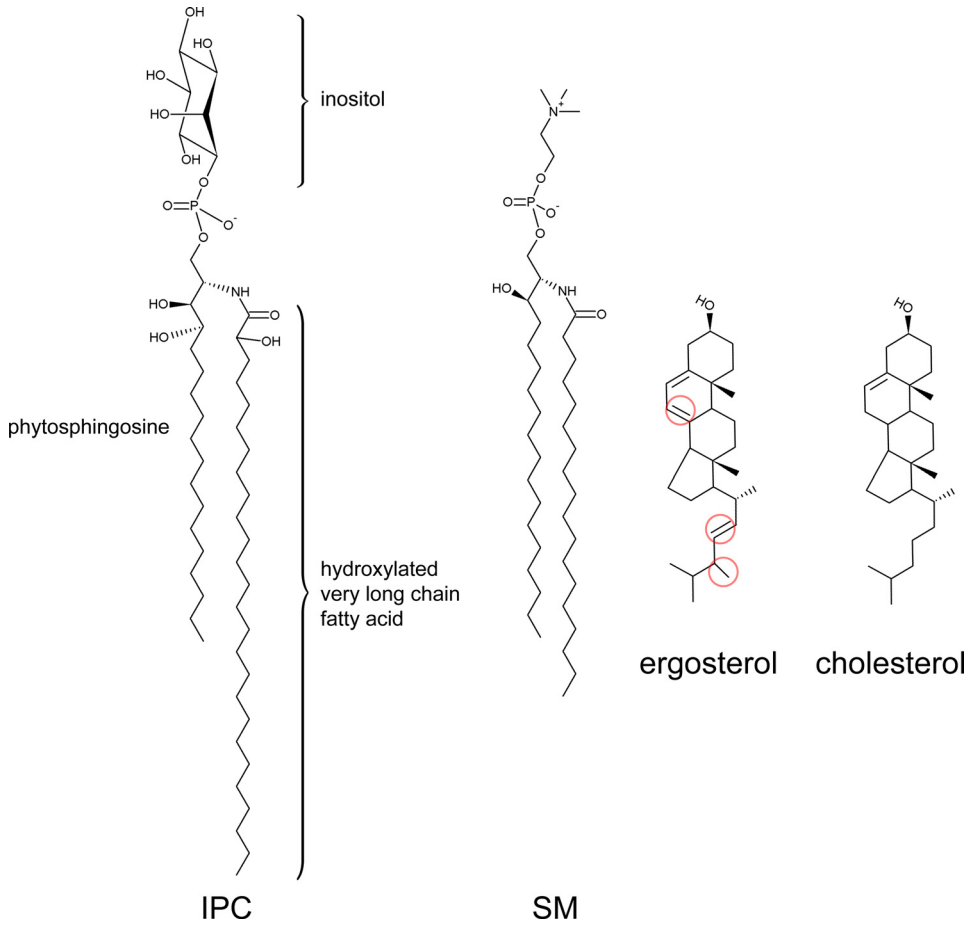

FIGURE 7. **Structural differences between yeast and mammalian sphingolipids and sterols.** Depicted are the structures of the major IPC species (IPC 18:0;3/26:0;1), C18-SM (*SM*), ergosterol, and cholesterol. Differences are highlighted and described in the text.

the very long chain fatty acid of IPC might lead to a hydrophobic mismatch between the IPC-rich Lo-like domain and the adjacent Ld-like domain (61). Third, asymmetric sphingolipids with very long chain fatty acids interdigitate into the opposing leaflet of the bilayer, even in the presence of a sterol, whereas the more symmetric yeast PI acyl chains are not expected to interdigitate (52, 62). This difference in acyl chain organization between an IPC-rich Lo-like phase and a PI-rich Ld-like phase might be an additional determinant for phase separation (53). Together, the differences in domain properties give rise to a high line tension at the domain boundaries, eventually leading to micrometer-scale phase separation to minimize domain boundaries.

The interactions between yeast sphingolipids (represented by IPC) and ergosterol in model membranes of simple composition can also give rise to phase separation in GUVs produced from a yeast total lipid extract (Fig. 1). As revealed by two-focus scanning FCS, the coexisting domains have Lo- and Ld-like properties. Furthermore, membrane order and phase separation depend on a proper sphingolipid composition because model membranes derived from total lipid extracts of mutants with defects in sphingolipid biosynthesis show reduced membrane order and fail to promote microscopic phase separation (Fig. 2). Thus, yeast lipids have the capacity to form domains even in membranes with complex compositions at ~23 °C, a temperature that is physiologically relevant for yeast cells. The yeast lipidome therefore has an inherent self-organizing potential, which provides a mechanistic basis for lipid sorting as recently demonstrated by the enrichment of sphingolipids and ergosterol in SVs and the consequent accumulation of these lipids in the plasma membrane (2, 27, 63). In agreement with this view, model membranes formed from yeast plasma membrane lipids are present in a single Lo-like phase.[4] The finding that model membranes formed from total lipid extracts of mutants with defective sphingolipid metabolism have a reduced order and fail to phase-separate microscopically has interesting implications for lipid raft-dependent protein transport in yeast. The mutants used here, *sur2*Δ and *elo3*Δ, have been shown to be defective for plasma membrane transport of integral membrane proteins (23, 24). It has been suggested that an aberrant membrane structure might be a reason for the observed effects (24). The altered properties of model membranes from *sur2*Δ and *elo3*Δ extracts support this notion (Fig. 2). Hence, the self-associative properties of yeast sphingolipids and ergosterol might facilitate both lipid and protein sorting into SVs.

Taken together, we provide direct evidence for membrane domain formation mediated by yeast sphingolipids and ergosterol. Yeast lipids thereby fulfill a key tenet of the lipid raft concept (5, 7, 8, 64). With this result, a comprehensive picture of raft-based lipid and protein sorting in yeast is emerging; sphingolipids and ergosterol are selectively sorted into secretory vesicles together with cargo protein destined to the plasma membrane (27). This process eventually results in the enrichment of these lipids at the plasma membrane (2, 63). During transport, yeast sphingolipids and ergosterol become detergent-resistant, and DRM association is required for proper localization of several *trans*-membrane proteins to the cell surface (18–21, 24, 25). These proteins lose DRM association in mutants with defective sphingolipid and/or ergosterol biosynthesis. Moreover, genes involved in sphingolipid and ergosterol biosynthesis interact genetically, indicating that these lipids also interact functionally (26, 60). The finding that yeast sphingolipids and ergosterol interact in membranes to form distinct fluid domains now provides a mechanistic framework for these indirect observations.

[4] C. Klose, D. Lingwood, H.-J. Kaiser, M. A. Surma, and K. Simons, unpublished data.

Acknowledgments—We are grateful to Robert Bittman and Bong Rae Cho for kindly providing reagents. We also thank Vyacheslav Zagoriy and Christoph Thiele for advice concerning the purification of yeast sphingolipids and Ilya Levental and Daniel Lingwood for helpful discussions.

REFERENCES

1. van Meer, G., Voelker, D. R., and Feigenson, G. W. (2008) *Nat. Rev. Mol. Cell Biol.* **9,** 112–124
2. Zinser, E., and Daum, G. (1995) *Yeast* **11,** 493–536
3. Simons, K., and van Meer, G. (1988) *Biochemistry* **27,** 6197–6202
4. De Matteis, M. A., and Luini, A. (2008) *Nat. Rev. Mol. Cell Biol.* **9,** 273–284
5. Simons, K., and Ikonen, E. (1997) *Nature* **387,** 569–572
6. Schuck, S., and Simons, K. (2004) *J. Cell Sci.* **117,** 5955–5964
7. Brown, D. A., and London, E. (1998) *Annu. Rev. Cell Dev. Biol.* **14,** 111–136
8. Lingwood, D., and Simons, K. (2010) *Science* **327,** 46–50
9. Jacobson, K., Mouritsen, O. G., and Anderson, R. G. W. (2007) *Nat. Cell Biol.* **9,** 7–14
10. Veatch, S. L., and Keller, S. L. (2002) *Phys. Rev. Lett.* **89,** 268101
11. Dietrich, C., Bagatolli, L. A., Volovyk, Z. N., Thompson, N. L., Levi, M., Jacobson, K., and Gratton, E. (2001) *Biophys. J.* **80,** 1417–1428
12. Ahmed, S. N., Brown, D. A., and London, E. (1997) *Biochemistry* **36,** 10944–10953
13. Schroeder, R., London, E., and Brown, D. (1994) *Proc. Natl. Acad. Sci. U.S.A.* **91,** 12130–12134
14. de Almeida, R. F., Fedorov, A., and Prieto, M. (2003) *Biophys. J.* **85,** 2406–2416
15. Simons, K., and Vaz, W. L. C. (2004) *Annu. Rev. Biophys. Biomol. Struct.* **33,** 269–295
16. Ipsen, J. H., Mouritsen, O. G., and Zuckermann, M. J. (1989) *Biophys. J.* **56,** 661–667
17. Ipsen, J. H., Karlström, G., Mouritsen, O. G., Wennerström, H., and Zuckermann, M. J. (1987) *Biochim. Biophys. Acta* **905,** 162–172
18. Lauwers, E., and André, B. (2006) *Traffic* **7,** 1045–1059
19. Bagnat, M., Keränen, S., Shevchenko, A., Shevchenko, A., and Simons, K. (2000) *Proc. Natl. Acad. Sci. U.S.A.* **97,** 3254–3259
20. Dupré, S., and Haguenauer-Tsapis, R. (2003) *Traffic* **4,** 83–96
21. Bagnat, M., Chang, A., and Simons, K. (2001) *Mol. Biol. Cell* **12,** 4129–4138
22. Lauwers, E., Grossmann, G., and André, B. (2007) *Mol. Biol. Cell* **18,** 3068–3080
23. Proszynski, T. J., Klemm, R. W., Gravert, M., Hsu, P. P., Gloor, Y., Wagner, J., Kozak, K., Grabner, H., Walzer, K., Bagnat, M., Simons, K., and Walch-Solimena, C. (2005) *Proc. Natl. Acad. Sci. U.S.A.* **102,** 17981–17986
24. Gaigg, B., Timischl, B., Corbino, L., and Schneiter, R. (2005) *J. Biol. Chem.* **280,** 22515–22522
25. Umebayashi, K., and Nakano, A. (2003) *J. Cell Biol.* **161,** 1117–1131
26. Guan, X. L., Souza, C. M., Pichler, H., Dewhurst, G., Schaad, O., Kajiwara, K., Wakabayashi, H., Ivanova, T., Castillon, G. A., Piccolis, M., Abe, F., Loewith, R., Funato, K., Wenk, M. R., and Riezman, H. (2009) *Mol. Biol. Cell* **20,** 2083–2095
27. Klemm, R. W., Ejsing, C. S., Surma, M. A., Kaiser, H. J., Gerl, M. J., Sampaio, J. L., de Robillard, Q., Ferguson, C., Proszynski, T. J., Shevchenko, A., and Simons, K. (2009) *J. Cell Biol.* **185,** 601–612
28. Ejsing, C. S., Sampaio, J. L., Surendranath, V., Duchoslav, E., Ekroos, K., Klemm, R. W., Simons, K., and Shevchenko, A. (2009) *Proc. Natl. Acad. Sci. U.S.A.* **106,** 2136–2141
29. Li, Z., Mintzer, E., and Bittman, R. (2006) *J. Org. Chem.* **71,** 1718–1721
30. Kim, H. M., Choo, H. J., Jung, S. Y., Ko, Y. G., Park, W. H., Jeon, S. J., Kim, C. H., Joo, T., and Cho, B. R. (2007) *Chembiochem* **8,** 553–559
31. García-Sáez, A. J., Carrer, D. C., and Schwille, P. (2010) *Methods Mol. Biol.* **606,** 493–508
32. Ries, J., and Schwille, P. (2006) *Biophys. J.* **91,** 1915–1924
33. Kaiser, H. J., Lingwood, D., Levental, I., Sampaio, J. L., Kalvodova, L., Rajendran, L., and Simons, K. (2009) *Proc. Natl. Acad. Sci. U.S.A.* **106,** 16645–16650
34. Kalvodova, L., Kahya, N., Schwille, P., Ehehalt, R., Verkade, P., Drechsel, D., and Simons, K. (2005) *J. Biol. Chem.* **280,** 36815–36823
35. Cheng, H. T., Megha, and London, E. (2009) *J. Biol. Chem.* **284,** 6079–6092
36. Baumgart, T., Hammond, A. T., Sengupta, P., Hess, S. T., Holowka, D. A., Baird, B. A., and Webb, W. W. (2007) *Proc. Natl. Acad. Sci. U.S.A.* **104,** 3165–3170
37. Lingwood, D., Ries, J., Schwille, P., and Simons, K. (2008) *Proc. Natl. Acad. Sci. U.S.A.* **105,** 10005–10010
38. Kahya, N., Scherfeld, D., Bacia, K., Poolman, B., and Schwille, P. (2003) *J. Biol. Chem.* **278,** 28109–28115
39. Oh, C. S., Toke, D. A., Mandala, S., and Martin, C. E. (1997) *J. Biol. Chem.* **272,** 17376–17384
40. Haak, D., Gable, K., Beeler, T., and Dunn, T. (1997) *J. Biol. Chem.* **272,** 29704–29710
41. Mouritsen, O. G. (2005) *Life – As a Matter of Fat: The Emerging Science of Lipidomics*, Springer, Berlin
42. Maulik, P. R., and Shipley, G. G. (1996) *Biophys. J.* **70,** 2256–2265
43. Stottrup, B. L., and Keller, S. L. (2006) *Biophys. J.* **90,** 3176–3183
44. Beattie, M. E., Veatch, S. L., Stottrup, B. L., and Keller, S. L. (2005) *Biophys. J.* **89,** 1760–1768
45. Xu, X., Bittman, R., Duportail, G., Heissler, D., Vilcheze, C., and London, E. (2001) *J. Biol. Chem.* **276,** 33540–33546
46. Urbina, J. A., Pekerar, S., Le, H. B., Patterson, J., Montez, B., and Oldfield, E. (1995) *Biochim. Biophys. Acta* **1238,** 163–176
47. Ramstedt, B., and Slotte, J. P. (2002) *FEBS Lett.* **531,** 33–37
48. Niemelä, P. S., Hyvönen, M. T., and Vattulainen, I. (2006) *Biophys. J.* **90,** 851–863
49. Boggs, J. M. (1987) *Biochim. Biophys. Acta* **906,** 353–404
50. Levental, I., Cebers, A., and Janmey, P. A. (2008) *J. Am. Chem. Soc.* **130,** 9025–9030
51. Björkbom, A., Ohvo-Rekilä, H., Kankaanpää, P., Nyholm, T. K., Westerlund, B., and Slotte, J. P. (2010) *Biochim. Biophys. Acta* **1798,** 453–460
52. Ruocco, M. J., Shipley, G. G., and Oldfield, E. (1983) *Biophys. J.* **43,** 91–101
53. McIntosh, T. J., Simon, S. A., Needham, D., and Huang, C. H. (1992) *Biochemistry* **31,** 2012–2020
54. Veiga, M. P., Arrondo, J. L., Goñi, F. M., Alonso, A., and Marsh, D. (2001) *Biochemistry* **40,** 2614–2622
55. Róg, T., and Pasenkiewicz-Gierula, M. (2006) *Biophys. J.* **91,** 3756–3767
56. Aittoniemi, J., Niemelä, P. S., Hyvönen, M. T., Karttunen, M., and Vattulainen, I. (2007) *Biophys. J.* **92,** 1125–1137
57. Guo, W., Kurze, V., Huber, T., Afdhal, N. H., Beyer, K., and Hamilton, J. A. (2002) *Biophys. J.* **83,** 1465–1478
58. Bloch, K. E. (1983) *CRC Crit. Rev. Biochem.* **14,** 47–92
59. Eisenkolb, M., Zenzmaier, C., Leitner, E., and Schneiter, R. (2002) *Mol. Biol. Cell* **13,** 4414–4428
60. García-Sáez, A. J., Chiantia, S., and Schwille, P. (2007) *J. Biol. Chem.* **282,** 33537–33544
61. Niemelä, P. S., Hyvönen, M. T., and Vattulainen, I. (2009) *Biochim. Biophys. Acta* **1788,** 122–135
62. Slater, J. L., and Huang, C. H. (1988) *Prog. Lipid Res.* **27,** 325–359
63. Hechtberger, P., and Daum, G. (1995) *FEBS Lett.* **367,** 201–204
64. Hancock, J. F. (2006) *Nat. Rev. Mol. Cell Biol.* **7,** 456–462